Structure
Article

Structural Basis for μ-Opioid Receptor Binding and Activation

Adrian W.R. Serohijos,[1,3,4] Shuangye Yin,[1] Feng Ding,[1] Josee Gauthier,[2] Dustin G. Gibson,[2] William Maixner,[2] Nikolay V. Dokholyan,[1,2,*] and Luda Diatchenko[2,*]
[1]Biochemistry and Biophysics Department
[2]Center for Neurosensory Disorders
[3]Physics and Astronomy Department
University of North Carolina at Chapel Hill, Chapel Hill, NC 27599, USA
[4]Present address: Department of Chemistry and Chemical Biology, Harvard University, Cambridge, MA 02138, USA
*Correspondence: dokh@med.unc.edu (N.V.D.), lbdiatch@email.unc.edu (L.D.)
DOI 10.1016/j.str.2011.08.003

SUMMARY

Opioids that stimulate the μ-opioid receptor (MOR1) are the most frequently prescribed and effective analgesics. Here we present a structural model of MOR1. Molecular dynamics simulations show a ligand-dependent increase in the conformational flexibility of the third intracellular loop that couples with the G protein complex. These simulations likewise identified residues that form frequent contacts with ligands. We validated the binding residues using site-directed mutagenesis coupled with radioligand binding and functional assays. The model was used to blindly screen a library of ~1.2 million compounds. From the 34 compounds predicted to be strong binders, the top three candidates were examined using biochemical assays. One compound showed high efficacy and potency. Post hoc testing revealed this compound to be nalmefene, a potent clinically used antagonist, thus further validating the model. In summary, the MOR1 model provides a tool for elucidating the structural mechanism of ligand-initiated cell signaling and for screening novel analgesics.

INTRODUCTION

Opioid analgesics are the most widely used drugs to treat moderate to severe pain (Inturrisi, 2002; Terrell et al., 2010). Mu-opioid receptors (MOR) in the peripheral and central nervous system are the primary target of exogenous opioid analgesics (Matthes et al., 1996; Reisine and Pasternak, 1996; Sora et al., 1997; Uhl et al., 1999). MOR agonists, such as morphine, exert their analgesic effects by stimulating MOR receptors leading to the initiation of presynaptic and postsynaptic inhibitory processes that decrease the electrical excitability and neurotransmitter release (Inturrisi, 2002; North, 1986; Reisine and Pasternak, 1996).

MOR receptors are members of the G protein-coupled receptor (GPCR) family. Canonical MOR signaling involves activation of inhibitory G-proteins ($G_{\alpha i/o}$) that leads to the dissociation of the heterotrimeric G protein complex. The release of the Gα subunit inhibits adenyl cyclase (AC) and the release of $G_{\beta\gamma}$ subunits activate K^+ channels and inhibit voltage-gated Ca^{2+} channels (VGCC) with AC-dependent decreases in cAMP levels being the most direct and immediate cellular event (Figure 1A) (Inturrisi, 2002; Reisine and Pasternak, 1996).

GPCRs are integral membrane proteins that exhibit conserved seven membrane-spanning helices, although the orientation of these helices may differ from one subfamily to another (Kobilka and Deupi, 2007). Because GPCRs are involved in major signal transduction pathways and also represent a major drug target, the modeling of their structure and function has been a major focus in the area of computational drug discovery (Ballesteros and Palczewski, 2001; Becker et al., 2004; Michino and Brooks, 2009). As such, three-dimensional modeling efforts have been applied to the major MOR isoform MOR1 (Alkorta and Loew, 1996; Filizola et al., 1999b; Filizola and Weinstein, 2002; Jordan and Devi, 1999; Strahs and Weinstein, 1997). Models of MOR1 (Alkorta and Loew, 1996; Filizola et al., 1999b; Strahs and Weinstein, 1997) have been constructed based on the X-ray structure of bovine rhodopsin (Palczewski et al., 2000), the first GPCR structure identified using X-ray crystallography. Although these models have been insightful, the further study of molecular dynamics (MD) that underlie ligand-receptor binding and the development of high throughput screening assays that will permit the identification of novel MOR ligands require higher resolution models. Moreover, understanding the structural basis of how MOR1 ligands engage G-proteins remains an open question.

In this study, we report the development of a high-resolution structural model of the MOR1. This structural model is in agreement with prior biochemical and pharmacological studies and is further confirmed using site-directed mutagenesis that identified critical ligand-binding residues. Molecular dynamics simulation of the receptor with and without morphine showed that the ligand binding leads to greater flexibility of the third intracellular loop, which is in agreement with the downstream protein complex interactions and signaling pathways activated by receptor agonists (Waldhoer et al., 2004). Finally, using our model, we have also conducted a virtual screening of a chemical library that consists of lead small molecular weight compounds to identify putative compounds that show strong binding to MOR1.

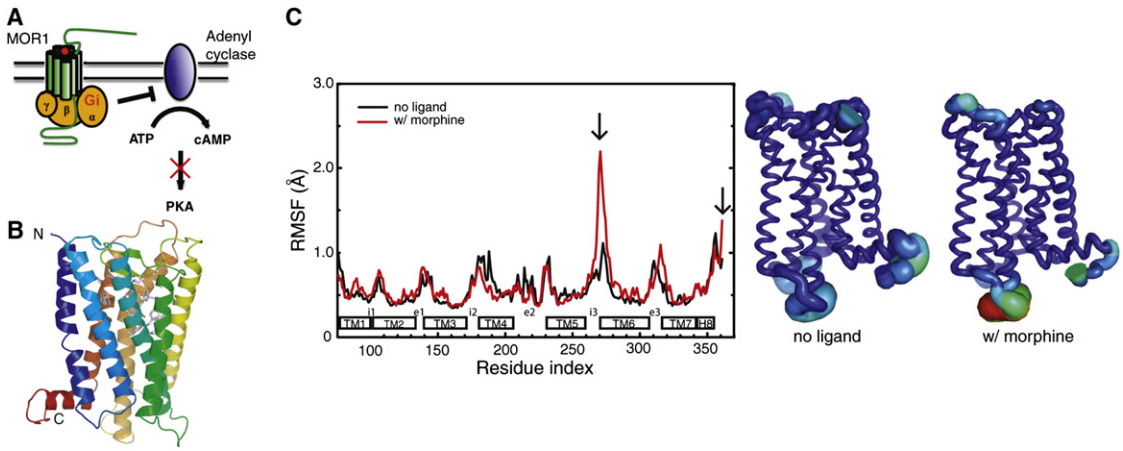

Figure 1. MOR1 Structural Model and Potential Mechanism for G Protein Activation

(A) Opioid drug binding to MOR1 activates the coupled G protein-effector, inhibiting adenyl cyclase, and downstream cAMP signaling cascades.

(B) Structural model of the receptor modeled from bovine rhodopsin exhibiting the seven-transmembrane topology conserved among GPCRs. N and C termini are colored blue and red, respectively.

(C) We performed MD simulation to investigate the stability and dynamics of the structure in the presence and absence of morphine. Plot of the per residue root-mean-square fluctuation (rmsf) to investigate the flexibility of various segments of the protein during the simulation. Arrows indicate the regions that change flexibility in the presence of morphine. The intra- and extracellular loops exhibit the greatest variability; most noteworthy are i3 and e3. The rmsf values are mapped into the protein structure. Backbone thickness and color is proportional to the rmsf values, thicker regions and warmer colors reflect greater flexibility whereas narrower regions and cooler colors reflect less flexibility.

See also Figure S1 and Table S1.

RESULTS

Structural Modeling and Effect of Ligands on Receptor Dynamics

GPCR structures exhibit seven transmembrane helices whose overall topological fold is conserved. We constructed preliminary structural models using five known crystal structures of GPCRs: bovine rhodopsin (Protein Data Bank [PDB] ID: 1u19), squid rhodopsin (PDB ID: 2z73), β1-adrenergic receptor (PDB ID: 2vt4), β2-adrenergic receptor (PDB ID: 2rhi), and A_{2A} adenosine receptor (PDB ID: 3eml) (see Experimental Procedures). The quality of the initial models was evaluated using Molprobity, which evaluates the accuracy of macromolecular structures through analysis of contacts and evaluation of dihedral angle combinations (Davis et al., 2007). Among the preliminary models, we found that the best candidate for further optimization to be the model constructed from bovine rhodopsin. This model was then revised to eliminate the invalid geometry, a procedure that was repeated until we arrived at a model whose backbone and side-chain geometry is comparable to GPCR crystal structures (Figure 1B; see Table S1 available online). We required the model accuracy be comparable to the experimental GPCR structures because of the strongly conserved topology of the protein especially in the transmembrane region. This requirement implies that the model is accurate enough for drug screening (see below). In the extracellular loop, we imposed that the model features the highly conserved disulfide bond between C142$^{3.36}$-C219 (numeric superscripts throughout the text indicate the Weinstein-Ballesteros convention of naming GPCR residues [Ballesteros and Weinstein, 1995]).

Additional validation of the model comes from docking morphine to the model structure and comparing the identified binding-pocket residues with prior mutagenesis and binding studies. To initially validate the residues that comprise the binding site, we mapped the sites to whose mutations have been shown previously to either affect or not affect morphine binding (Figure S1). For example, mutating D116$^{2.50}$ in (TM2) to asparagine and Y328$^{7.43}$ (TM7) to phenylalanine has shown to significantly reduce morphine-binding by 100- to 1000-fold (Raynor et al., 1994; Surratt et al., 1994). As shown in the model, D116$^{2.50}$ and Y328$^{7.43}$ mediate morphine binding in the putative binding site. Known mutations in the protein that do not significantly influence ligand binding are generally either far or have side chains pointing away from the ligand-binding pocket, suggesting that they may not be as critical in forming the binding pocket (Figure S1B). These mutations include V128A$^{2.62}$ in TM2; T139E$^{3.23}$, I140L$^{3.24}$, I146A/L$^{3.30}$, and N152A$^{3.36}$ in TM3; I200V$^{4.56}$ and V204I$^{4.60}$ in TM4; K235R/A/H/L$^{5.39}$ in TM5; and H299Q/N$^{6.52}$ in TM6. The putative binding pocket was further validated by our own mutagenesis studies (see below).

To evaluate the structural integrity of the model, we performed all-atom MD simulation of the model structure in GROMACS (Lindahl et al., 2001) using a modified Gromos96 force field for the protein, lipid, and morphine (Chandrasekhar et al., 2003; Oostenbrink et al., 2005; Schüttelkopf and van Aalten, 2004) (see Experimental Procedures for details). Indeed, from the 20 ns of equilibrium MD simulation, we observed that the protein is stable with root-mean-square deviation (rmsd) stabilized within 3.5 Å, indicating no major structural clashes or unnatural protein interactions in the model (Figure S2). Such values of equilibrium rmsd have also been observed in simulations of GPCR structures derived from X-ray, such as bovine rhodopsin (Schlegel et al., 2005) and A_{2A} adrenergic receptor

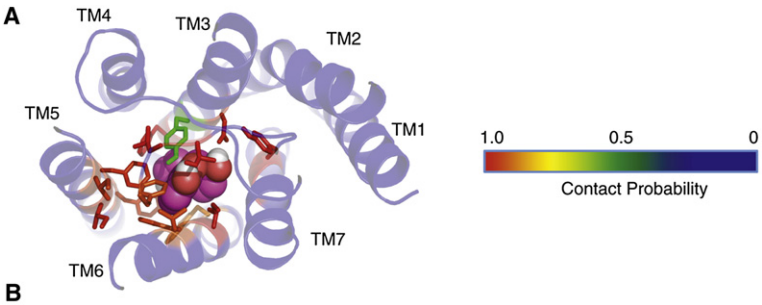

B

Mutated Residues	Location	Mutant Description	K_d binding (nM)	K_d F.C.	Bmax	EC_{50} cAMP (nM)	EC_{50} F.C
T220G	e2	Remove polar and non-polar interactions	0.54 ± 0.1	0.66	4601 ± 499	10.8 ± 1.8	0.80
L221S	e2	Disrupt hydrophobic interactions	2.54 ± 0.3**	3.13	1491 ± 184	197.7 ± 44.5**	14.59
F223A	e2	Large to small hydrophobic residue	3.15 ± 0.4 **	3.89	8692 ± 879	33.4 ± 8.7*	2.47
I240A$^{5.44}$	TM5	Large to small hydrophobic residue	1.10 ± 0.1	1.36	5057 ± 427	28.9 ± 7.4	2.13
D149A$^{3.33}$	TM3	Remove polar interactions	4.67 ± 0.8**	5.77	2053 ± 315	N.A.	
M153S$^{3.37}$	TM3	Disrupt hydrophobic interactions	63.1 ± 16.3**	77.9	3959 ± 1242	796.2 ± 309.1**	58.75
W295H$^{6.48}$	TM6	Perturbation of the conserved tryptophan	15.14 ± 2.5**	18.69	4935 ± 881	1088.9 ± 705.3**	80.35
I298A$^{6.51}$	TM6	Reduce hydrophobic interactions	4.05 ± 0.7**	5	1757 ± 278	1094.0 ± 647.3**	80.72
V302A$^{6.55}$	TM6	Reduce hydrophobic interactions	2.74 ± 0.3**	3.38	5952 ± 669	59.0 ± 19.9*	4.36
WT-MOR1			0.81 ± 0.07		4094 ± 164	13.6 ± 2.1	1

Figure 2. Binding Pocket of MOR1 Receptor and Targeted Mutagenesis

(A) Shown are residues within the 4.5 Å of the bound morphine. Side chains are colored according to their contact probability, which is defined as the likelihood of interacting with morphine during the simulation run. Contact probability of 1 indicates that the specific residue is always within 4.5 Å of morphine, whereas 0 indicates that the residue is always beyond 4.5 Å of morphine.

(B) To validate the predicted residues near the binding site, we choose mutations that were predicted to disrupt morphine and diprenorphine binding. The receptor locations of the mutated residues are listed, TM is coded for helix and e is coded for extra-cellular loop. **$p < 0.0001$ and *$p < 0.05$ different from MOR1 WT. Numeric superscripts indicate the Weinstein-Ballesteros convention of naming GPCR residues (Ballesteros and Weinstein, 1995).

See also Figure S2 and Table S3.

(Rodríguez et al., 2011), and typically indicate structural relaxation to a minimum energy state.

We next computed the average root-mean-square fluctuations of each residue, which quantifies the local conformational flexibility (Figure 1C). Expectedly, the extracellular and intracellular loop regions are the most flexible and the membrane-embedded regions are the least flexible. The most dynamic regions are the third intracellular loop i3 and C terminus of the receptor, which has also been shown to be very flexible from comparison of various experimental structures of other GPCR proteins (Cherezov et al., 2007; Jaakola et al., 2008; Murakami and Kouyama, 2008; Rosenbaum et al., 2007; Spivak et al., 1997; Warne et al., 2008). The increased flexibility of the loop i3 observed in our simulation of MOR1 may be related to the rearrangement of helices TM5 and TM6 (both connected by i3) in the adrenergic receptor as this GPCR switches from active to inactive conformation (Rasmussen et al., 2011).

To investigate the effects of bound ligands on the equilibrium dynamics of the receptor, we performed a similar simulation of the MOR1 structure with bound morphine. We found that the presence of ligand dramatically changed the flexibility of the i3 region and the distal end of the C terminus (Figure 1C), consistent with the critical role of both the i3 and the C terminus in G protein binding and cell signaling (Hanson and Stevens, 2009; Waldhoer et al., 2004; Milligan and White, 2001).

Identifying Residues Critical for Ligand Binding

In order to utilize the in silico structural model to identify high-affinity ligands using structure-based drug screening methods, it is crucial to accurately model the ligand binding pocket of the receptor. From the MD simulations of MOR1 receptor with morphine, a widely clinically used opioid agonist, we identified the residues that have high frequency contacts with the ligand (Figure 2A). We surmise that these residues are critical for the ligand binding. To validate these predictions and the model, we generated single residue mutants to perturb interaction with morphine (Figure 2B). All mutations were designed to be conservative, with the goal of substantially diminishing ligand binding without affecting the overall protein folding or processing (Figure 2B).

We then experimentally characterized the ligand binding properties of the receptor mutants and their sensitivity to morphine-dependent cAMP inhibition (Figures 2B and 3). Mutation-dependent changes in ligand affinity were assessed by determining the K_d values of corresponding mutants obtained using a homologous competition binding assay with 1 nM [^{3}H]diprenorphine. [^{3}H]Diprenorphine was chosen as a probe because it is structurally similar to morphine and it is be insensitive to any alterations in constitutive receptor-G protein coupling caused by the mutations. Compared to morphine, the model predicted that diprenorphine showed similar residues with high frequency contacts.

To assess changes in morphine potency due to mutations, we determined the EC_{50} values obtained via a bioluminescent assay that measured morphine dose-dependent inhibition of intracellular cAMP levels using a cAMP-sensitive luciferase reporter. Inhibition of stimulated cAMP production was chosen as a most direct functional assay to measure the morphine-dependent

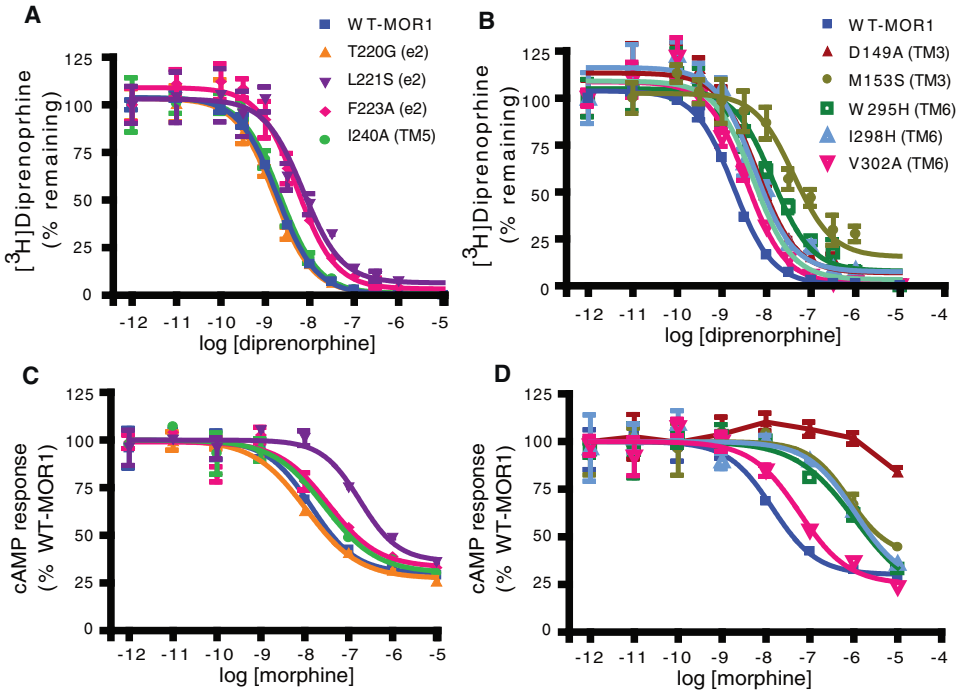

Figure 3. Binding Affinity and Potency of MOR1 Mutants

HEK293T cells transiently transfected with MOR1 wild-type (WT-MOR1) or MOR1 mutants expressing constructs were subjected to (A and B) competitive radioligand binding assay or (C and D) cAMP-sensitive luciferase reporter assay. The effect of mutations specific for e2 and TM5 domains (A and C) are shown separately from the effect of mutations specific for TM3 and TM6 domains (B and D). (A and B) Increasing concentrations of MOR1 antagonist diprenorphine, ranging from 10^{-14} to 10^{-12} M were applied with uniform 1 nM ^{3}H-diprenorphine to determine K_d for each mutant and K_d fold change (F.C.) relative to WT-MOR1. Statistically significant fold changes in K_d ranged from 3.13 (L221S) to 77.9 (M153S). (C and D) Increasing concentrations of morphine, ranging from 10^{-14} to 10^{-12} M were applied to isoproterenol (100 nM) pretreated cells to inhibit cAMP production and determine EC_{50} and EC_{50} fold-change (F.C) relative to WT-MOR1. Cotreatment of morphine with MOR1 antagonist naloxone damped the inhibitory effect of morphine. Significant fold-changes in EC_{50} ranged from 2.47 (F223A) to 80.72 (I298A). N/A: cAMP assay was failing due to very low baseline cAMP levels.

activation of MOR1-$G\alpha_{i/o}$ complex and subsequent inhibition of AC (Inturrisi, 2002; Reisine and Pasternak, 1996) (Figures 1 and 3).

Compared to wild-type (WT-MOR1), the K_d values of the receptor mutants decreased up to 78-fold (M153S$^{3.37}$). Similarly, EC_{50} values exhibited up to 80-fold decrease (I298A$^{6.51}$) in efficacy. In general, we observed strong correlation between changes in K_d and EC_{50} values in all mutants except one, which shows stronger affect on potency. The B_{max} for all the mutants showed comparable values suggesting no effect on receptor expression. Comparison of the K_d and EC_{50} values for WT-MOR1 with the K_d and EC_{50} values for the mutants in the TM3 and TM6 revealed most robust reduction in ligand binding and morphine potency. Two of the three mutants in the e2 loop (L221S, F223A) also show significantly weaker ligand binding compared to WT-MOR1 (~3 fold difference in K_d values and 15- and 2.5-fold difference in EC_{50} values, respectively). The observed effect of e2 point mutations were more modest than those in the transmembrane helices, this is probably due to the greater conformational flexibility of e2 loop compared to the TM helices (Figure 1C). A greater conformational flexibility would allow conformational rearrangement to accommodate the ligand, thus dampening the effects of the mutation. Thus, our ability to detect any significant effects is supportive of the correct mapping of the contact residues L221S and F223A and model in general. It is also noteworthy that in the published structures of rhodopsin, adrenergic, and adenosine GPCRs, the e2 loop is topologically divergent, highlighting a potential important role for the e2 loop in dictating ligand specificity.

In contrast, the I240A mutation in TM5 did not significantly alter ligand affinity and potency, suggesting that the sequence of TM5 during the homology modeling was possibly misaligned and is consistent with the fact that sequence alignment can be a challenge in homology modeling. Alternatively, it is plausible that the I240A mutation was too conservative to significantly perturb ligand binding, thus a less conservative mutation at the 5.44 locus would better reveal whether I240 participates in morphine binding as predicted in the model.

Virtual Screening for MOR1 Binding Ligands

Using the MOR1 structure models, we then computationally screened a chemical compound library consisting of 1,296,388 ZINC compounds (Irwin and Shoichet, 2005) for novel ligands predicted to bind the MOR1 receptor (Figure 4A). We computationally docked each compound onto the MOR1 structure and estimated its binding affinity based on docking poses. To select the best hits, we first ranked all compounds based on the predicted binding affinities and then visually inspected the electrostatic contacts of the top 100 compounds. The criteria for

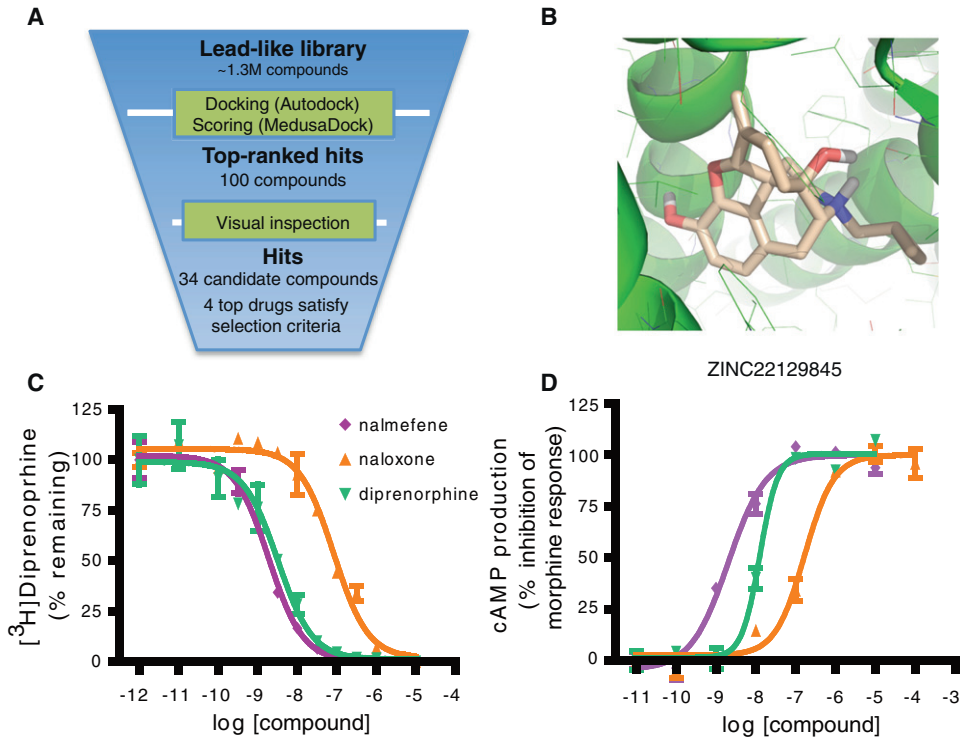

Figure 4. Virtual Screening and Binding Affinity and Potency of Nalmefene

(A) We screened a library of ~1.3 M compounds (ZINC) (Irwin and Shoichet, 2005) using the MOR1 model and Autodock (Morris et al., 2009). We visually inspected the docking poses of the top scoring ligands and select the ligands that have reasonable poses and electrostatic contact with the target.

(B) We found several target hits that include opioid-like compounds such as (nalmefene [Revex], ZINC22129845).

(C and D) HEK293 cells transiently transfected with MOR1 expressing constructs were subjected to (C) competitive radioligand binding assay or (D) cAMP-sensitive luciferase reporter assay. (C) Increasing concentrations of nalmefene, diprenorphine, and naloxone were applied with uniform 1 nM ^{3}H-diprenorphine to determine K_i. The K_i for nalmefene, diprenorphine, and naloxone are 1.303, 2.128, and 57.40 nM, respectively, which are statistically different from each other ($p < 0.0002$). (D) Cells were then treated with 100 nM isoproterenol and 1 μM morphine for another 10 min. EC_{50} values for nalmefene, diprenorphine and naloxone are 2.05 nM, 12.64 nM, and 168.00 nM, which are statistically different from each other ($p < 0.0001$).

See also Table S2 and Table S4.

selection also included binding energy predictions, the number of rotatable bonds, and the cluster size of the docking poses. Ligands with smaller number of rotatable bonds have less entropic penalty upon binding, whereas those with larger cluster size of docking poses are dynamically more favorable. We took extra account of these effects because they are not included in the original binding energy prediction. Our final selection included four ligands that satisfy all criteria and additional 30 ligands that ranked top according to electrostatic matching, number of rotatable bonds, or cluster size. Out of these four selected ligands, three were available from commercial sources (Table S2). We screened these three compounds for both binding affinity and receptor potency using receptor binding and cAMP inhibition assays. One of these three compounds (ZINC22129845) showed strong binding (K_i = 1.303 nM) and antagonist properties (IC_{50} = 11.28 nM, in the presence of 1 μM of morphine). Post hoc testing revealed this compound to be nalmefene (Revex), a recent potent opioid receptor antagonist that is used in the clinical setting (Figure 4). The blind identification of a known potent MOR1 antagonist further validates the accuracy of the binding pocket predicted by the model. Importantly, we would like to stress that even though we identified a known opioid antagonist, our study was not retrospective, because we identified this compound in an unbiased screening using formal criteria.

We inspected the docking poses of all 34 ligands and observed that the ligand-binding sites are located between TM3, TM5, TM6, and TM7. Although the binding site location is consistent with our knowledge of other GPCR structures, the detailed binding motif associated with our model is quite different. The major interaction of the docking poses is the salt-bridge between the amine group and an aspartate in TM3, and hydrophobic interaction with TM5, TM6, and TM7. The binding pose is also deeper into the receptor than the known binding motif in rhodopsin, β1-adrenergic receptor, β2-adrenergic receptor, and A_{2A} adenosine receptor (Hanson and Stevens, 2009). The deeper binding pose associated with MOR1, when compared with other GPCR ligands, permits small compounds like morphine to penetrate deeper into the binding pocket.

We also reevaluated the binding affinity of some known MOR ligands using a flexible-receptor docking and scoring protocol (Ding et al. 2010; Yin et al., 2008). We used MedusaScore (Yin et al., 2008) to approximate the binding energy for nalmefene, which resulted in a predicted MedusaScore of −51.6 kcal/mol.

Nalmefene was ranked first among the four hits that satisfy all the criteria for best docking energies (Table S2). In comparison, the predicted MedusaScore for morphine is −44.3 kcal/mol. We also calculated the predicted MedusaScore for two other widely used MOR1 antagonists, naloxone and diprenorphine, as well as experimentally identified their K_d and IC_{50} values relative to nalmefene. The MedusaScore for naloxone was −50.3 kcal. The lower MedusaScore of diprenorphine (−62.2 kcal/mol) compared to nalmefene (−51.6 kcal/mol) is due to a larger clash energy (37.9 kcal/mol for diprenorphine and 17.8 kcal/mol for nalmefene), which is not included in MedusaScore. The MedusaScore difference between naloxone and nalmefene qualitatively agrees with the experimental observation of their binding potency and efficacy (Figures 4C and 4D), confirming the superior potency of nalmefene. Furthermore, nalmefene showed significantly greater binding and potency than both naloxone and diprenorphine (Figures 4C and 4D).

To verify the robustness of our model to discriminateMOR1 ligands from non-ligands, we examined if there are other known MOR1 ligands in the library apart from nalmefene. We searched the screening library for compounds similar to morphine with a Tanimoto coefficient >0.5, and found 21 morphine analogs (Table S4). Tanimoto coefficient measures the similarity between two compounds based on the presence or absence of molecular fragments (Shivakumar and Krauthammer, 2009). We then used the structures of these morphine analogs to query PubChem and the ZINC database for their biological activities. We found that among the morphine analogs, nalmephene was the only known MOR1 ligand among them. This result is not surprising because we used a ''lead-like'' compound library for screening whereas most MOR ligands are not ''lead-like.'' Notably three compounds (ZINC22065588, ZINC16940005, and ZINC17130997) were identified that are chemically more similar to morphine than nalmefene, yet they are not known to bind MOR1. Our virtual screening also ranked them much lower than nalmefene, which further demonstrates the capability of our structural model to discriminate putative MOR1 ligands from non-MOR1 ligands.

DISCUSSION

MOR1 is a major pharmacological target for opioid analgesics, yet our knowledge related to this receptor's structure and mechanisms of activation and signaling are limited. In addition to the basic molecular biological and pharmacological significance, our findings are of clinical importance because >30% of patients treated with opioids report inadequate pain relief (Ballantyne and Shin, 2008; Noble et al., 2010) and thus the search for effective and safe opioids remains a pressing clinical need. The production of an accurate and detailed receptor model is one of the first necessary steps in this endeavor. Key questions include determining the map of receptor-ligand interactions as well as the structural mechanism by which a receptor switches from a quiescent to an active state and transmit extracellular signals to intracellular effectors. Modeling receptor structure and dynamics is crucial if we are to adequately address these key questions.

GPCR modeling efforts have been applied to MOR1 previously (Alkorta and Loew, 1996; Filizola et al., 1999b; Filizola and Weinstein, 2002; Strahs and Weinstein, 1997). Filizola et al. (1999a, 1999b) constructed a homology model of the MOR1 receptor using the rhodopsin structure and performed a 500-ps unconstrained MD simulation to relax and evaluate the stability of the structure. Although the model correctly suggested that the MOR1 binding cavity is located in an inner inter-helical region constituted by transmembrane helices TM3, TM4, TM5, TM6, and TM7, and is partially covered by dynamic extracellular loops, the accuracy of the model was limited by the availability of mutational studies, short MD simulation, and absence of models of the extra- and intracellular loops (Filizola et al., 1999b). More recently, Zhang et al. (2005) constructed another homology model of the MOR1 receptor, also from rhodopsin, and performed a 2-ns MD simulation using a membrane-aqueous system. Liu et al. (2009) also used MD simulation to study the potential binding modes of several endomorphics. These modeling efforts have been insightful but did not examine the effects of ligand binding on receptor dynamics, a crucial issue in understanding receptor function.

To address these critical issues, we built a new structural model of the MOR1 receptor using the bovine rhodopsin receptor. The model agrees with prior mutational studies on the MOR1 receptor (Figure S1). In addition, we generated a predictive interaction map between the ligand and the receptor, which we subsequently validated experimentally by targeted mutagenesis (Figures 2 and 3). All but two mutations we identified and tested significantly reduced ligand potency and efficacy, illustrating the accuracy of our in silico predictive model.

To investigate the structural mechanism by which ligand binding to the receptor is transformed into cellular signaling, we performed simulations of the receptor dynamics in the absence and presence of ligand (Figure 1C). We found that the flexibility of intracellular loop i3 dramatically changes when morphine is bound to the receptor, consistent with the critical role of i3 as the docking site of G-proteins binding. The increased flexibility of i3 morphine-bound state could serve as a structural activator or a ''mechanical signal'' coupling the receptor and G protein, which further initiates the signaling cascade as proposed in earlier experimental studies (Hanson and Stevens, 2009; Waldhoer et al., 2004). Although the role of i3 in coupling the receptor and the G protein has been known, the molecular structural details of how this coupling arises in the absence or presence of ligand was unknown. Furthermore, morphine-dependent modulation of C terminus flexibility is also in agreement with the critical role of C terminus in GPCRs signaling as a structural site for phosphorylation and a binding site for scaffolding proteins (Milligan and White, 2001). Thus, our results provide a structural basis for the MOR1 ligand initiated signaling and a tool to study these structural mechanisms. Furthermore, whereas other GPCRs vary in the length and conformation of their i3 and C terminus, the structural basis of their activation upon ligand binding could be a universal mechanism.

We also used the model structure to virtually screen ~1.3 million compounds in the ZINC library for novel MOR1 ligands (Figure 4). Among the top hits (Rank 1; Table S2), we blindly identified a morphine-like compound (nalmefene) that has potent MOR1 binding and antagonistic properties, validating our model of the binding pocket. Using this model receptor-drug complex, we computationally predicted the binding affinities of nalmefene, naloxone and morphine to be −55.7 kcal/mol, −49.3 kcal/mol, and −42.3 kcal/mol, respectively, all in qualitative agreement

with the experimentally observed efficacy of these three drugs, further confirming the accuracy of the model. Additionally, nalmefene, one of the 34 hits identified in the high throughput computational screen and one of the three compounds screened in the cellular assays, showed very strong binding characteristics to the build MOR1model and was a stronger antagonist of MOR1 than naloxone and diprenorphine (Figures 4C and 4D). This finding suggests that further screening of the selected compounds is likely to yield other high potency MOR1 ligands.

In summary, we have constructed a structural model of MOR1 opioid receptor of high resolution and accuracy. The employment of MD simulations allowed us to show a morphine-dependent increase in i3 intracellular loop flexibility and to determine residues that have high frequency contacts with MOR1 ligands. Subsequent use of the developed MOR1 structure model to computationally screen a large chemical compound library yielded a number of novel ligands predicted to bind the receptor with high potency. Thus, our results offered new structural insights in MOR1 ligand binding and receptor activation and provided a tool for both studying the structural mechanism of MOR1 ligand initiated cell signaling and in silico screening for novel opioids that can produce high potency analgesia.

EXPERIMENTAL PROCEDURES

Structural Modeling and Molecular Dynamics Simulation

We used CLUSTALW to determine initial sequence alignment between human MOR1 (Accession ID: P35372) and GPCR templates, bovine rhodopsin (PDB ID: 1u19), squid rhodopsin (PDB ID: 2z73), β1-adrenergic receptor (PDB ID: 2vt4), β2-adrenergic receptor (PDB ID: 2rhi), and A_{2A} adenosine receptor (PDB ID: 3eml). Model construction was performed in the MODELER suite of InsightII (Accelrys, San Diego). Models were evaluated for correct protein geometry using Molprobity. The model building and evaluation was performed recursively until we arrived at reasonable models of MOR1 (Table S2).

We performed MD simulations using GROMACS (Lindahl et al., 2001) with the Gromos96 force field modified with additional parameters for lipids and morphine (Chandrasekhar et al., 2003; Oostenbrink et al., 2005; Schüttelkopf and van Aalten, 2004). We used explicit model for water SPC. We used genbox to embed the MOR1 receptor in a pre-equilibrated DPPC bilayer. To ensure the packing of lipids around the receptor, we initially imposed harmonic constraints (force constant 1000 kJ $mol^{-1}nm^{-2}$) on the receptor and performed short 0.5 ns simulation run to equilibrate the lipids. The force constant is sequentially lowered to 500 kJ $mol^{-1}nm^{-2}$, 200 kJ $mol^{-1}nm^{-2}$, and 100 kJ $mol^{-1}nm^{-2}$, each time performing a short 0.5 ns simulation. Finally, we performed a production run of 20 ns without constraints. Long-range electrostatics is treated with Particle Mesh Ewald with a grid spacing of 12 Å and a cutoff of 10 Å.

Drug Screening

We screened the clean-lead subset of ZINC database retrieved on January 23, 2009. This subset contains 1,296,388 compound structures in ready-to-dock format. For the receptor structure used in the docking, we used a conformation derived from MD simulations with morphine bound. Specifically, we clustered the MD derived snapshots and used the centroid of the largest cluster. We applied Autodock4 for docking calculation, which uses genetic algorithm (GA) and force field-based scoring function to search for best binding poses (Morris et al., 2009). We prepared the docking grid and parameters using AutoDockTools (Morris et al., 2009). We used the default docking parameters except for the number of maximum GA evaluations (increased to 1,750,000) and the size of GA population (increased to 150). For each molecule, we generated 30 docking poses and assigned the one with lowest binding energy as the final docking pose. We tested the parameters by redocking the morphine molecules to recapitulate the pose observed in the MD simulation. The screening was performed in a Linux cluster using ~500 CPU nodes in average (the Topsail cluster in University of North Carolina at Chapel Hill).

Binding and cAMP Assays

Mutants were generated by overlapping polymerase chain reaction approach. Radioligand binding assays were performed using established protocols (Huang et al., 2009). Briefly, membrane preparations containing recombinant receptor were incubated with [^{3}H]diprenorphine in the presence of varying concentrations of putative ligand. After 1 hr, assays were harvested onto Wallac GF/A filtermats using a Filtermate harvester (Perkin Elmer). Then, Meltilex scintillant (Wallac) were melted onto dried filtermats and residual bound radioligand were measured by scintillation counting in TriLux microbeta counter (Wallac). Monitoring of intracellular cAMP levels were performed using the GloSensor cAMP-sensitive luciferase reporter (Promega). Briefly, cells coexpressing GloSensor-22F and receptor isoforms were seeded in white, 384-well plates for 24 hr. The next day, the medium were replaced with GloSensor reagent (Promega), and incubated for 2 hr. Then, cells were challenged with morphine at various concentrations. After 5 min, the cells were stimulated with 100 nM isoproterenol and luminescence was read on a Victor^3 (Perkin Elmer) plate counter. When antagonist treatment is done, cells were pretreated with the antagonist compounds for 30 min prior to morphine and isoproterenol treatment.

SUPPLEMENTAL INFORMATION

Supplemental Information includes two figures and four tables and can be found with this article online at doi:10.1016/j.str.2011.08.003.

ACKNOWLEDGMENTS

This work was supported in part by NIH/NIDCR, NIH/NINDS, and NIH/NCRR grants RO1-DE16558 (L.D. and W.M.), UO1-DE017018 (W.M. and L.D.), NS41670 (W.M.), PO1 NS045685 (W.M. and L.D.), R01GM080742 (N.V.D.), the ARRA supplement 3R01GM080742-03S1 (N.V.D.), and research funds from Algynomics Inc. and Molecules in Action, Inc. The authors thank Brian Roth and Vincent Setola and the NIMH Psychoactive Drug Screening Program (PDSP) at UNC for materials and their assistance in performing assays and analyzing data. The authors likewise thank Oskar Laur for the generation of receptor mutants.

Received: March 28, 2011
Revised: July 13, 2011
Accepted: August 4, 2011
Published: November 8, 2011

REFERENCES

Alkorta, I., and Loew, G.H. (1996). A 3D model of the delta opioid receptor and ligand-receptor complexes. Protein Eng. *9*, 573–583.

Ballantyne, J.C., and Shin, N.S. (2008). Efficacy of opioids for chronic pain: a review of the evidence. Clin. J. Pain *24*, 469–478.

Ballesteros, J., and Palczewski, K. (2001). G protein-coupled receptor drug discovery: implications from the crystal structure of rhodopsin. Curr. Opin. Drug Discov. Devel. *4*, 561–574.

Ballesteros, J.A., and Weinstein, H. (1995). Integrated methods for the construction of three dimensional models and computational probing of structure-function relations in G-protein coupled receptors. Methods Neurosci. *25*, 366–428.

Becker, O.M., Marantz, Y., Shacham, S., Inbal, B., Heifetz, A., Kalid, O., Bar-Haim, S., Warshaviak, D., Fichman, M., and Noiman, S. (2004). G protein-coupled receptors: in silico drug discovery in 3D. Proc. Natl. Acad. Sci. USA *101*, 11304–11309.

Chandrasekhar, I., Kastenholz, M., Lins, R.D., Oostenbrink, C., Schuler, L.D., Tieleman, D.P., and van Gunsteren, W.F. (2003). A consistent potential energy parameter set for lipids: dipalmitoylphosphatidylcholine as a benchmark of the GROMOS96 45A3 force field. Eur. Biophys. J. *32*, 67–77.

Cherezov, V., Rosenbaum, D.M., Hanson, M.A., Rasmussen, S.G., Thian, F.S., Kobilka, T.S., Choi, H.J., Kuhn, P., Weis, W.I., Kobilka, B.K., and Stevens, R.C. (2007). High-resolution crystal structure of an engineered human beta2-adrenergic G protein-coupled receptor. Science *318*, 1258–1265.

Davis, I.W., Leaver-Fay, A., Chen, V.B., Block, J.N., Kapral, G.J., Wang, X., Murray, L.W., Arendall, W.B., 3rd, Snoeyink, J., Richardson, J.S., and Richardson, D.C. (2007). MolProbity: all-atom contacts and structure validation for proteins and nucleic acids. Nucleic Acids Res. *35* (Web Server issue), W375–W383.

Ding, F., Yin, S., and Dokholyan, N.V. (2010). Rapid flexible docking using a stochastic rotamer library of ligands. J. Chem. Inf. Model. *50*, 1623–1632.

Filizola, M., Carteni-Farina, M., and Perez, J.J. (1999a). Molecular modeling study of the differential ligand-receptor interaction at the mu, delta and kappa opioid receptors. J. Comput. Aided Mol. Des. *13*, 397–407.

Filizola, M., and Weinstein, H. (2002). Structural models for dimerization of G-protein coupled receptors: the opioid receptor homodimers. Biopolymers *66*, 317–325.

Filizola, M., Laakkonen, L., and Loew, G.H. (1999b). 3D modeling, ligand binding and activation studies of the cloned mouse delta, mu; and kappa opioid receptors. Protein Eng. *12*, 927–942.

Hanson, M.A., and Stevens, R.C. (2009). Discovery of new GPCR biology: one receptor structure at a time. Structure *17*, 8–14.

Huang, X.P., Setola, V., Yadav, P.N., Allen, J.A., Rogan, S.C., Hanson, B.J., Revankar, C., Robers, M., Doucette, C., and Roth, B.L. (2009). Parallel functional activity profiling reveals valvulopathogens are potent 5-hydroxytryptamine(2B) receptor agonists: implications for drug safety assessment. Mol. Pharmacol. *76*, 710–722.

Inturrisi, C.E. (2002). Clinical pharmacology of opioids for pain. Clin. J. Pain ***18*** (4, Suppl), S3–S13.

Irwin, J.J., and Shoichet, B.K. (2005). ZINC—a free database of commercially available compounds for virtual screening. J. Chem. Inf. Model. *45*, 177–182.

Jaakola, V.P., Griffith, M.T., Hanson, M.A., Cherezov, V., Chien, E.Y., Lane, J.R., Ijzerman, A.P., and Stevens, R.C. (2008). The 2.6 angstrom crystal structure of a human A2A adenosine receptor bound to an antagonist. Science *322*, 1211–1217.

Jordan, B.A., and Devi, L.A. (1999). G-protein-coupled receptor heterodimerization modulates receptor function. Nature *399*, 697–700.

Kobilka, B.K., and Deupi, X. (2007). Conformational complexity of G-protein-coupled receptors. Trends Pharmacol. Sci. *28*, 397–406.

Lindahl, E., Hess, B., and van der Spoel, D. (2001). GROMACS 3.0: a package for molecular simulation and trajectory analysis (Berlin, Heidelberg: Springer), pp. 306–317.

Liu, X., Kai, M., Jin, L., and Wang, R. (2009). Molecular modeling studies to predict the possible binding modes of endomorphin analogs in mu opioid receptor. Bioorg. Med. Chem. Lett. *19*, 5387–5391.

Matthes, H.W., Maldonado, R., Simonin, F., Valverde, O., Slowe, S., Kitchen, I., Befort, K., Dierich, A., Le Meur, M., Dollé, P., et al. (1996). Loss of morphine-induced analgesia, reward effect and withdrawal symptoms in mice lacking the mu-opioid-receptor gene. Nature *383*, 819–823.

Michino, M., and Brooks, C.L., III. (2009). Predicting structurally conserved contacts for homologous proteins using sequence conservation filters. Proteins *77*, 448–453.

Milligan, G., and White, J.H. (2001). Protein-protein interactions at G-protein-coupled receptors. Trends Pharmacol. Sci. *22*, 513–518.

Morris, G.M., Huey, R., Lindstrom, W., Sanner, M.F., Belew, R.K., Goodsell, D.S., and Olson, A.J. (2009). AutoDock4 and AutoDockTools4: Automated docking with selective receptor flexibility. J. Comput. Chem. *30*, 2785–2791.

Murakami, M., and Kouyama, T. (2008). Crystal structure of squid rhodopsin. Nature *453*, 363–367.

Noble, M., Treadwell, J.R., Tregear, S.J., Coates, V.H., Wiffen, P.J., Akafomo, C., and Schoelles, K.M. (2010). Long-term opioid management for chronic noncancer pain. Cochrane Database Syst. Rev. *Jan 20(1)*, CD006605.

North, R.A. (1986). Membrane conductances and opioid receptor subtypes. NIDA Res. Monogr. *71*, 81–88.

Oostenbrink, C., Soares, T.A., van der Vegt, N.F., and van Gunsteren, W.F. (2005). Validation of the 53A6 GROMOS force field. Eur. Biophys. J. *34*, 273–284.

Palczewski, K., Kumasaka, T., Hori, T., Behnke, C.A., Motoshima, H., Fox, B.A., Le Trong, I., Teller, D.C., Okada, T., Stenkamp, R.E., et al. (2000). Crystal structure of rhodopsin: A G protein-coupled receptor. Science *289*, 739–745.

Rasmussen, S.G., Choi, H.J., Fung, J.J., Pardon, E., Casarosa, P., Chae, P.S., Devree, B.T., Rosenbaum, D.M., Thian, F.S., Kobilka, T.S., et al. (2011). Structure of a nanobody-stabilized active state of the β(2) adrenoceptor. Nature *469*, 175–180.

Raynor, K., Kong, H., Chen, Y., Yasuda, K., Yu, L., Bell, G.I., and Reisine, T. (1994). Pharmacological characterization of the cloned kappa-, delta-, and mu-opioid receptors. Mol. Pharmacol. *45*, 330–334.

Reisine, T., and Pasternak, G. (1996). Opioid analgesics and antagonists. In The Pharmacological Basis of Therapeutics, A.G. Gilman, L.S. Goodman, and A. Gilman, eds. (New York: McGraw-Hill), pp. 528–532.

Rodríguez, D., Piñeiro, A., and Gutiérrez-de-Terán, H. (2011). Molecular dynamics simulations reveal insights into key structural elements of adenosine receptors. Biochemistry *50*, 4194–4208.

Rosenbaum, D.M., Cherezov, V., Hanson, M.A., Rasmussen, S.G., Thian, F.S., Kobilka, T.S., Choi, H.J., Yao, X.J., Weis, W.I., Stevens, R.C., and Kobilka, B.K. (2007). GPCR engineering yields high-resolution structural insights into beta2-adrenergic receptor function. Science *318*, 1266–1273.

Schlegel, B., Sippl, W., and Höltje, H.D. (2005). Molecular dynamics simulations of bovine rhodopsin: influence of protonation states and different membrane-mimicking environments. J. Mol. Model. *12*, 49–64.

Schüttelkopf, A.W., and van Aalten, D.M.F. (2004). PRODRG: a tool for high-throughput crystallography of protein-ligand complexes. Acta Crystallogr. D Biol. Crystallogr. *60*, 1355–1363.

Shivakumar, P., and Krauthammer, M. (2009). Structural similarity assessment for drug sensitivity prediction in cancer. BMC Bioinformatics *10* (*Suppl 9*), S17.

Sora, I., Takahashi, N., Funada, M., Ujike, H., Revay, R.S., Donovan, D.M., Miner, L.L., and Uhl, G.R. (1997). Opiate receptor knockout mice define mu receptor roles in endogenous nociceptive responses and morphine-induced analgesia. Proc. Natl. Acad. Sci. USA *94*, 1544–1549.

Spivak, C.E., Beglan, C.L., Seidleck, B.K., Hirshbein, L.D., Blaschak, C.J., Uhl, G.R., and Surratt, C.K. (1997). Naloxone activation of mu-opioid receptors mutated at a histidine residue lining the opioid binding cavity. Mol. Pharmacol. *52*, 983–992.

Strahs, D., and Weinstein, H. (1997). Comparative modeling and molecular dynamics studies of the delta, kappa and mu opioid receptors. Protein Eng. *10*, 1019–1038.

Surratt, C.K., Johnson, P.S., Moriwaki, A., Seidleck, B.K., Blaschak, C.J., Wang, J.B., and Uhl, G.R. (1994). -mu opiate receptor. Charged transmembrane domain amino acids are critical for agonist recognition and intrinsic activity. J. Biol. Chem. *269*, 20548–20553.

Terrell, K.M., Hui, S.L., Castelluccio, P., Kroenke, K., McGrath, R.B., and Miller, D.K. (2010). Analgesic prescribing for patients who are discharged from an emergency department. Pain Med. *11*, 1072–1077.

Uhl, G.R., Sora, I., and Wang, Z. (1999). The mu opiate receptor as a candidate gene for pain: polymorphisms, variations in expression, nociception, and opiate responses. Proc. Natl. Acad. Sci. USA *96*, 7752–7755.

Waldhoer, M., Bartlett, S.E., and Whistler, J.L. (2004). Opioid receptors. Annu. Rev. Biochem. *73*, 953–990.

Warne, T., Serrano-Vega, M.J., Baker, J.G., Moukhametzianov, R., Edwards, P.C., Henderson, R., Leslie, A.G., Tate, C.G., and Schertler, G.F. (2008). Structure of a beta1-adrenergic G-protein-coupled receptor. Nature *454*, 486–491.

Yin, S., Biedermannova, L., Vondrasek, J., and Dokholyan, N.V. (2008). MedusaScore: an accurate force field-based scoring function for virtual drug screening. J. Chem. Inf. Model. *48*, 1656–1662.

Zhang, Y., Wang, D., Johnson, A.D., Papp, A.C., and Sadée, W. (2005). Allelic expression imbalance of human mu opioid receptor (OPRM1) caused by variant A118G. J. Biol. Chem. *280*, 32618–32624.

